J. Fluid Mech. (2003), *vol.* 497, *pp.* 319–334.
DOI: 10.1017/S0022112003006669 Printed in the United Kingdom

On buoyant plumes rising from area sources in a calm environment

By T. K. FANNELØP[1] AND D. M. WEBBER[2]

[1]E+E Flow Analysis, Utsikten 6, N-3179 Åsgårdstrand, Norway

[2]Integral Science and Software Ltd, 484 Warrington Rd., Culcheth, Warrington WA3 5RA, UK

(Received 17 June 2002 and in revised form 3 July 2003)

Low-momentum releases of buoyant material from area sources are investigated in the context of the model of Morton, Taylor & Turner (1956) (MTT). The general solution of the model equations is shown to include the case of a converging–diverging flow which we have used to model plumes from the area sources. These solutions have as asymptotes certain power solutions in terms of height, i.e. the MTT solution at large heights and a non-entraining solution near the source. The new solutions exhibit distinct and interesting flow features such as a neck (point of minimum cross-section) and a velocity peak somewhat above. The new results have been compared with the few known experimental data sources and reasonable agreement is demonstrated. In the process we have also examined the importance of the Boussinesq approximation and find results recently published not to be valid except in one special case.

1. Introduction

Morton, Taylor & Turner's (1956) solutions for plumes and thermals were limited to isolated sources of buoyancy and small differences in density, or to a region well above the source where air entrainment has brought the plume density sufficiently close to the ambient value. Later extensions to line sources, thermals, forced plumes and puffs had similar limitations. Over time these solutions have proved useful in a large variety of applications, not only in geophysics, but also in engineering and environmental problems.

More recently (e.g. Rooney & Linden 1996; Martin *et al.* 1997) it has been observed that derivation of the MTT model rests on assumptions of self-similarity, but not necessarily of small density differences. This extends the region of applicability of the model closer to a source where the density difference may be considerable, e.g. fire and natural gas plumes. Rooney & Linden (1996) have demonstrated that larger density differences primarily influence the plume radius and that the velocity is largely unchanged from the Boussinesq value, but here we shall show that this conclusion is dependent on a very particular choice of entrainment model.

Real sources have finite area and, in extending the region under investigation to closer to the source, one must consider the validity of the (virtual) point source assumption which is often made (e.g. Morton *et al.* 1956; Turner 1973; Rooney & Linden 1996). The point source model may be sufficient to describe the plume in the region high above the source but, as we shall see, in general it is inadequate closer to the (real) source. In particular it cannot describe the lower regions of a plume from an area source which accelerates upwards and contracts to a neck, above which it decelerates and expands to an asymptotic form matching that described by Morton

et al. (MTT). Here we shall show that the MTT model equations may provide much more information about this region if one abandons the virtual point source assumption. (Not all solutions of the equations have a 'point' source – a location where the plume has zero radius. For those that do, it must be a 'virtual' one on extrapolation of the solution below the physical region where the solution applies.)

2. The model

The MTT model describes a steady plume rising in a calm atmosphere in terms of its characteristic radius $b(z)$, upward velocity $w(z)$, and density $\rho(z)$ as a function of vertical coordinate z. Equivalently one may transform to mass, momentum, and buoyancy fluxes $q(z)$, $f(z)$, $\phi(z)$, which we shall define, for convenience, modulo factors of π, gravitational acceleration g, and ambient air density ρ_a, by

$$q \equiv \eta w b^2, \quad f \equiv \eta w^2 b^2, \quad \phi \equiv (1-\eta) w b^2, \tag{2.1}$$

where $\eta \equiv \rho/\rho_a$ is the density ratio. For reference the inverse transformation is

$$\frac{\rho}{\rho_a} \equiv \eta \equiv \frac{q}{q+\phi}, \quad b \equiv \sqrt{\frac{q(q+\phi)}{f}}, \quad w \equiv \frac{f}{q}. \tag{2.2}$$

The model equations for mass, momentum, and species (or buoyancy) conservation, expressed equivalently in terms of each set of variables, are

$$\frac{\mathrm{d}}{\mathrm{d}z}\eta w b^2 = 2 b u_E, \quad \frac{\mathrm{d}q}{\mathrm{d}z} = 2 u_E \sqrt{\frac{q(q+\phi)}{f}}, \tag{2.3}$$

$$\frac{\mathrm{d}}{\mathrm{d}z}\eta w^2 b^2 = g(1-\eta) b^2, \quad \frac{\mathrm{d}f}{\mathrm{d}z} = [g\phi]\frac{q}{f}, \tag{2.4}$$

$$\frac{\mathrm{d}}{\mathrm{d}z}(1-\eta) w b^2 = 0, \quad \frac{\mathrm{d}\phi}{\mathrm{d}z} = 0 \tag{2.5}$$

(see e.g. Turner 1973; Fanneløp 1994). Here u_E is an entrainment velocity which we shall write as

$$u_E = \alpha w \sqrt{\eta} k(\eta) \tag{2.6}$$

on dimensional grounds. Here α is a dimensionless entrainment coefficient and $k(\eta)$, which we define so that $k(1) = 1$, is an arbitrary function of the density ratio. The two most popular entrainment models are those of MTT ($k(\eta) \equiv 1/\sqrt{\eta}$) (see also Taylor 1958) and Ricou & Spalding (1961) ($k(\eta) \equiv 1$).

3. Dimensions and self-similarity

The conserved buoyancy flux ϕ (see (2.5)) and the acceleration due to gravity, g, provide a 'buoyancy length scale' L and 'buoyancy velocity scale' U defined by

$$L \equiv \left[\frac{\phi^2}{g}\right]^{1/5}, \quad U \equiv [g^2\phi]^{1/5} \quad \text{or} \quad \phi \equiv L^2 U, \quad g \equiv \frac{U^2}{L}. \tag{3.1}$$

The assumption of self-similarity in the derivation of the model is essentially that there are no other important length and velocity scales, and that various cylindrically symmetric fields denoted by a which are functions of radial coordinate r and vertical coordinate z may be expressed in the form $a(z, r/b(z))$ where b is the characteristic

plume radius. In this way the radial dependence of a has the same profile at different heights but with a different characteristic radius $b(z)$. In the absence of the length scale L it could be argued on dimensional grounds that $b(z) \sim z$, and in fact this is the asymptotic (large-z) form of the solutions as long as $\alpha > 0$. However the existence of the scale L makes the general solution more interesting.

Also of interest from dimensional considerations is the (densimetric) Froude number $Fr = w/[g(1-\eta)b]^{1/2}$ or $Fr = (1+\phi/q)^{1/4}(f^{5/4})(g\phi q^2)^{-1/2}$. Asymptotically or in the Boussinesq regime ($q \gg \phi$) this simplifies significantly to $Fr \sim (U^3 L)^{-1/2}(f^{5/4}/q)$ but more generally is much more complicated owing to the existence of the scales L and U. It is important to note that once the assumption of self-similarity has been made in the derivation of the plume equations, it has no further part to play in their solution, but also that it will almost always break down sufficiently close to a real source, whose radius provides a second length scale which may be important in that region. We shall discuss this latter point in more detail below in some particular cases.

4. The general solution of the plume equations

4.1. *General considerations*

A common approach to solving equations of this kind is to assume that various quantities behave simply as powers of z, substitute power laws, and solve for the exponents. Alternatively, and essentially equivalently, a virtual point source is assumed. However this procedure misses non-power-law solutions, which in this case are very instructive. Therefore let us consider the general solution of the mass, momentum and species equations given above, without making any further assumptions. In general, this can be given formally (though not necessarily explicitly) as follows. First, the buoyancy is conserved

$$\phi = \text{constant}. \tag{4.1}$$

Second, the ratio of mass and momentum equations gives a separable form with a solution for $q(f)$ obtainable (formally) from

$$\int \mathrm{d}q q k \left(\frac{q}{q+\phi} \right) = \frac{2\alpha}{g\phi} \int f^{3/2}\, \mathrm{d}f. \tag{4.2}$$

Third, once $q(f)$ has been found, then $z(f)$ can also be found from the momentum equation:

$$z = \frac{1}{[g\phi]} \int \frac{f}{q(f)}\, \mathrm{d}f. \tag{4.3}$$

This results in relationships between the various variables treating f as the independent parameter. Webber, Jones & Tickle (1997) used q as the independent variable, but using f has the technical advantage that it is always monotonic in z, whereas q ceases to be so in the limit $\alpha \to 0$.

It is now 'simply' a matter of solving some algebraic equations to find $q(z)$, $f(z)$, after which the inverse transform given above yields $\eta(z)$, $w(z)$, $b(z)$. In general there are three constants of integration which are determined by initial conditions for three independent variables. One is the conserved buoyancy flux ϕ, the second is an interesting one from the mass integral which we shall discuss below, and the third, from the momentum integral, is simply a choice of origin of z.

To proceed further we need to define the entrainment models of practical interest (by specifying the function k).

4.2. *The Ricou–Spalding entrainment model* ($k = 1$)

It is immediately apparent that the Ricou–Spalding model (where $k = 1$) will be the simplest to pursue mathematically. In this case the mass integral gives

$$q = \sqrt{q_0^2 + \left[\frac{8\alpha}{5g\phi}\right] f^{5/2}}, \tag{4.4}$$

where q_0 is the constant of integration†, representing the mass flux at the (virtual) point where the momentum flux f is zero. It is also worth noting that this is approximately true for other entrainment models in the limit $q \gg \phi$. Solving for z is less tractable. The result is

$$z = \frac{1}{[g\phi]} \int \frac{f}{\sqrt{q_0^2 + [8\alpha/5g\phi] f^{5/2}}}\, \mathrm{d}f, \tag{4.5}$$

which may only be expressed in closed form in terms of special functions which are sufficiently obscure to be generally unhelpful.

However one particular subset of solutions is particularly simple – the family defined by $q_0 = 0$. In this case, and only in this case (for $\alpha \neq 0$), one obtains $f(z - z_0)$ and $q(z - z_0)$ as power laws. The solution for $q_0 = 0$ is

$$f(z) \to F \cdot \left[\tfrac{9}{10}\alpha\right]^{2/3} \left(\frac{z - z_0}{L}\right)^{4/3}, \quad q \to \phi \tfrac{4}{3} \left[\tfrac{9}{10}\alpha\right]^{4/3} \left(\frac{z - z_0}{L}\right)^{5/3}, \tag{4.6}$$

where L is the buoyancy length scale and $F \equiv L^2U^2 \equiv [\phi/L]^2$. Given that f and q behave as powers of $(z - z_0)$ it is clear from the above analysis that the quantities

$$\frac{\rho_a - \rho}{\rho} \equiv \frac{(1 - \eta)}{\eta} \equiv \frac{\phi}{q}, \quad w \equiv \frac{f}{q}, \quad b\sqrt{\frac{\rho}{\rho_\alpha}} \equiv \sqrt{\frac{q}{f}} \tag{4.7}$$

will all do so too. In particular there is a point source ($b = 0$) at $z = z_0$.

In fact if one assumes this power dependence (or the existence of a point source) in attempting to derive a solution, then this one with $q_0 = 0$ is the only one which will be found for $\alpha \neq 0$. We note that the above power-law expressions are also valid as large-z (large-f, large-q) asymptotes of all solutions with $\alpha \neq 0$. However, the non-power-law solutions are very interesting physically, as we shall see.

4.3. *The Morton–Taylor–Turner entrainment model* (*MTT*)

The solution of the MTT model, defined by $k(\eta) \equiv 1/\sqrt{\eta}$, proceeds the same way in principle. This time the mass integral relating q and f yields the somewhat less manageable form

$$\begin{aligned}[(q + 3\phi/2)\sqrt{q(q + \phi)} - (q_0 + 3\phi/2)\sqrt{q_0(q_0 + \phi)}] \\ - \frac{3\phi^2}{2} \ln\left[\frac{\sqrt{q} + \sqrt{(q + \phi)}}{\sqrt{q_0} + \sqrt{(q_0 + \phi)}}\right] = \left[\frac{8\alpha}{5g\phi}\right] f^{5/2},\end{aligned} \tag{4.8}$$

where again the constant of integration is represented by the terms involving q_0, which is defined as the mass flux at the point where $f = 0$. Although in principle this

† Note also that q_0^2 may be replaced by a negative number, but here we are specifically interested in the properties of plumes $q_0^2 \geqslant 0$. These are the eponymous lazy plumes of Hunt & Kaye (2001).

implies a function $q(f)$, the z-dependence given by

$$z = \frac{1}{[g\phi]} \int \frac{f}{q(f)}\, \mathrm{d}f \tag{4.9}$$

is now even less likely to give a useful closed analytic expression. We can however observe that $q_0 = 0$ does not yield a simple power-law dependence $q(f)$ as it did for Ricou–Spalding entrainment, and nor does any other value of q_0. A power-law dependence of the velocity $w = f/q$ on z will also not result (except as an approximation in the Boussinesq limit – or as a large-z asymptote, which is effectively saying the same thing).

5. Properties of the general solution of the entraining models

Despite the lack of a full, general, explicit, analytic solution for $b(z)$ etc. a number of properties of the general solution are readily ascertained as follows.

5.1. *Necking*

Many of the solutions of the plume equations will exhibit a 'neck' – a point of minimum radius as illustrated schematically in figure 1. Associated with this is a point of maximum velocity, below which the flow is accelerating and above which it is decelerating. This is not quite at the same height as the minimum radius, but rather the velocity is maximum where $b\sqrt{(\rho_a - \rho)}$ is minimum, as is implied by the conserved buoyancy flux.

The point of maximum velocity

The rate of change of $w = f/q$ with height z is readily found to be

$$\frac{\mathrm{d}w}{\mathrm{d}z} = \frac{1}{q}\left[1 - \frac{2\alpha k}{g\phi}\frac{f^{5/2}}{q^2}\right]\frac{\mathrm{d}f}{\mathrm{d}z}. \tag{5.1}$$

Asymptotically, at large height (and everywhere in the power-law solution of the Ricou–Spalding model) this becomes

$$\frac{\mathrm{d}w}{\mathrm{d}z} \xrightarrow[z\to\infty]{} -\frac{[g\phi]}{4f}. \tag{5.2}$$

The velocity w is seen to decrease with height.

The non-power-law solutions originate from a virtual source with $f = 0, q \neq 0$ ($w = 0$) and will therefore accelerate initially, and achieve a maximum velocity before the asymptotic deceleration sets in. In fact, at the virtual source location the solution is singular with $b \to \infty$, $\mathrm{d}b/\mathrm{d}z \to -\infty$, $\mathrm{d}w/\mathrm{d}z \to \infty$.

It follows that there is therefore a location on the solution (which may or may not lie above the source in the physical region) where w is a maximum. Defining this as $z = z_w$, we have

$$\left.\frac{2\alpha k}{g\phi}\frac{f^{5/2}}{q^2}\right|_{z_w} = 1. \tag{5.3}$$

For the Ricou–Spalding model solution discussed above this is where $q^2 = 5q_0^2$, i.e. the height where entrainment has resulted in a total mass flux which is $\sqrt{5}$ times its value at the virtual source of infinite area.

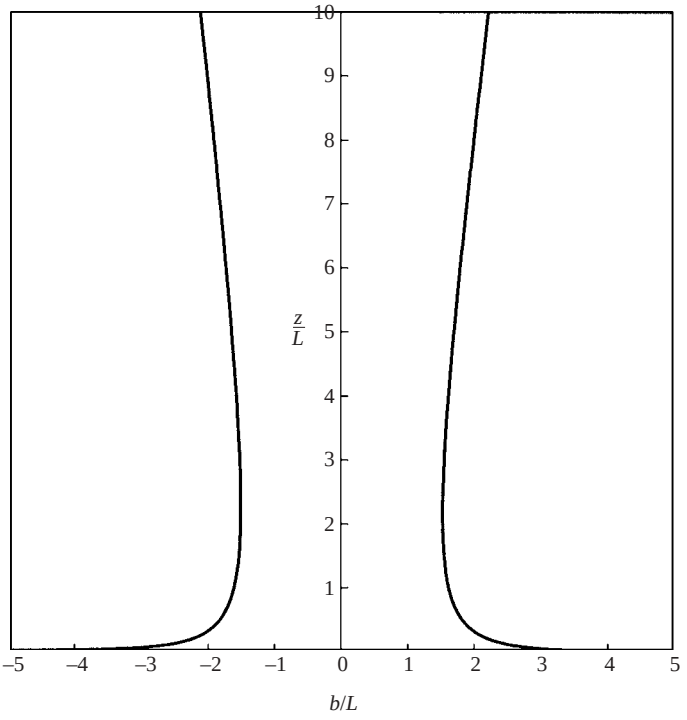

FIGURE 1. A side view of a predicted converging–diverging plume from an area source. The radius b and height z are shown in dimensionless units based on the buoyancy length scale L defined in the text. This example – source conditions $(b, w, \eta) = (5\,\mathrm{m},\ 0.2\,\mathrm{m\,s^{-1}},\ 0.6)$ – has dimensionless velocity $w/U = 0.07$ at ground level, and uses the Morton–Taylor–Turner entrainment model with $\alpha = 0.1$. One may question the precise validity of the entraining plume equations in the very sharply converging region near the ground, but in fact the entrainment there is very small (as the velocity is very small) and so the profile closely reproduces the Bernoulli profile in this region (as we discuss in § 5.3) and this lends confidence to the overall result.

The point of minimum radius (*the neck*)

The point of minimum radius can be found in the same way, by considering the rate of change of the cross-sectional area $b^2 = q(q+\phi)/f$ with the momentum flux f. This is found to be

$$\frac{\mathrm{d}b^2}{\mathrm{d}z} = \frac{q(q+\phi)}{f^2}\left[\frac{2\alpha(1+\eta)k}{g\phi}\frac{f^{5/2}}{q^2} - 1\right]\frac{\mathrm{d}f}{\mathrm{d}z}. \tag{5.4}$$

Asymptotically at large height (large values of f and q) this becomes (for $\alpha \neq 0$)

$$\frac{\mathrm{d}b^2}{\mathrm{d}z} \xrightarrow[z\to\infty]{} \frac{3}{2}\frac{[g\phi]q^2(q+\phi)}{f^3}, \tag{5.5}$$

and therefore, high in the plume, the radius increases with height. Again, in all but the power-law solution, the virtual source with $f = 0, q \neq 0$ implies the existence of a region where radius is decreasing with height, and hence, somewhere between, a point of minimum radius. Again, depending on the source conditions, this point may or may not be in the physical region, above the ground. If it is, then there is a neck.

The neck, at height z_b say, is found where

$$\left.\frac{2\alpha(1+\eta)k}{g\phi}\frac{f^{5/2}}{q^2}\right|_{z_b} = 1. \tag{5.6}$$

It is also clear that, at the point of maximum velocity, the radius b is increasing with z. Thus the maximum velocity must always occur above the neck.

Finally let us observe that the expression for $\mathrm{d}b^2/\mathrm{d}z$ may be estimated at the ground from the source conditions (even though one may be concerned about the self-similarity assumption here). Immediately above a source with small enough momentum, and/or a small enough entrainment coefficient, the plume will decrease in radius. In fact one may use this as a practical criterion of what is meant by a 'low-momentum source' of a buoyant plume.

The existence of a neck thus drops very simply out of the theory. Below we shall discuss it in the context of laboratory experiments, but in addition the neck is seen in field observations of cold or burning light-gas plumes from large-scale underwater releases of natural gas. Fanneløp, Hirschberg & Kueffer (1991) reproduce a photograph of such a plume, showing a strong inflow towards the centre near the ocean surface, the formation of a neck, and large-scale instability and transition to turbulence above the neck region.

5.2. *The Boussinesq limit*

The Boussinesq region is defined as that where $(1-\eta) \ll 1$ or $q \gg \phi$. In this region $k(\eta) \sim 1$ and the flux equations for all the entrainment models discussed reduce to those of the Ricou–Spalding model. This provides an asymptotic ($z \to \infty$) description of the plume. At first sight, this invites a very peculiar conclusion, for the resultant equations (for any of the models considered) reduce to the Ricou–Spalding model. Put another way, if we start with the Ricou–Spalding model, then the flux equations for q, f, ϕ are completely unchanged by making the Boussinesq approximation. So are we thus to conclude that the Boussinesq approximation is completely irrelevant for this model?

The answer is of course 'no'. For whilst the differential flux equations (in the Ricou-Spalding model) are unchanged in the Boussinesq approximation, the transformations back to the primitive variables do change:

$$\left.\begin{aligned} &\frac{\rho_a-\rho}{\rho_a} \equiv 1-\eta \equiv \frac{\phi}{q+\phi} \to \frac{\phi}{q}, \\ &b \equiv \sqrt{\frac{q(q+\phi)}{f}} \to \frac{q}{\sqrt{f}}, \\ &w \equiv \frac{f}{q} \to \frac{f}{q}. \end{aligned}\right\} \tag{5.7}$$

The exception here is the velocity, whose expression in terms of the fluxes does not change in the Boussinesq limit. This simple property lies at the heart of Rooney & Linden's (1996) observation that non-Boussinesq effects affect the radius but not the velocity. In fact we can go further than this and note that whilst this feature is a property of the Ricou–Spalding entrainment model, it will not be true in general where $k(\eta) \neq 1$. For in that case, making the Boussinesq approximation does not leave the flux equations invariant. The solution for $q(z)$, $f(z)$ will in general be different from the Boussinesq approximate solution, and that difference will be seen also in the velocity. We discuss this further below.

We conclude that the flux equations for the Boussinesq and Ricou–Spalding models of an entraining plume are mathematically entirely equivalent. Thus for example, for any solution $(1-\eta_B, b_B, w_B)$ of the Boussinesq limit, there is a solution $(1-\eta_{RS}, b_{RS}, w_{RS})$ of the Ricou–Spalding model which can be simply found from the transformation

$$\bar{\eta}_{RS} = \bar{\eta}\frac{1}{(1+\bar{\eta}_B)}, \quad b_{RS} = b_B\sqrt{1+\bar{\eta}_B}, \quad w_{RS} = w_B, \tag{5.8}$$

where $\bar{\eta} \equiv 1-\eta \equiv (\rho_a - \rho)/\rho$ must be evaluated in the Boussinesq approximation from the buoyancy flux. Whilst the Boussinesq limit of all entraining models discussed here is the same, this property is a unique feature of the Ricou–Spalding model.

It is also perhaps worth emphasizing that the Boussinesq limit does not preclude plume solutions with a neck. The analysis which led to the possibility of a converging plume from a low-momentum source is equally valid for a source of gas close to ambient density.

To round off our analysis of non-Boussinesq effects with a general entrainment velocity, let us return to the original model description in terms of w, b, η and look, following Rooney & Linden, at the approach to the Boussinesq limit. To this effect we write

$$\eta(z) = 1-\varepsilon(z), \quad b(z) = b_0(z)[1+B_1\varepsilon], \quad w(z) = w_0(z)[1+W_1\varepsilon] \tag{5.9}$$

and look for an approximate solution where ε is small everywhere. The density dependence of the entrainment velocity may be expanded as

$$\sqrt{\eta}k(\eta) = 1 - J_1\varepsilon + O(\varepsilon^2) \tag{5.10}$$

with $J_1 = 0$ for Morton–Taylor–Turner entrainment and $J_1 = 1/2$ for Ricou–Spalding. For current purposes we shall look at the solution which results in simple powers of z in the Boussinesq limit. Keeping the buoyancy flux finite but otherwise taking $\varepsilon \to 0$ in the traditional manner gives the Boussinesq result

$$b_0(z) = B_0 z, \quad w_0(z) = W_0 z^{-1/3}, \tag{5.11}$$

with constants

$$B_0 = \frac{6\alpha}{5}, \quad W_0 = \left[\frac{3[g\phi]}{4}\left(\frac{5}{6\alpha}\right)^2\right]^{1/3}. \tag{5.12}$$

At the next order in ε, the conserved buoyancy tells us that

$$\varepsilon(z) \cong \varepsilon_0 z^{-5/3} \quad \text{with} \quad \varepsilon_0 = \frac{\phi}{W_0 B_0^2}. \tag{5.13}$$

Using these lowest-order solutions, substituting in the mass and momentum equations we obtain the next-order solution in the form given above, as long as

$$B_1 = \frac{2J_1+1}{4}, \quad W_1 = \frac{2J_1-1}{4}. \tag{5.14}$$

We therefore find that the velocity w *is* sensitive to non-Boussinesq effects at first order, except for the case $J_1 = 1/2$, i.e. the Ricou–Spalding case. This perturbation analysis shows, therefore, that there is such an effect except in the case of a very specific entrainment model, but cannot of course show, as we have done above that the absence of an effect in the Ricou–Spalding model is true to all orders in all solutions. Rooney & Linden's conclusion that the velocity was insensitive to non-Boussinesq effects was based on a calculation which assumed a power-law solution. But, as we

have observed, power-law solutions only exist as a subset of the solutions for the Ricou–Spalding entrainment model, and therefore the assumption of such a solution focuses automatically on that entrainment model and on that particular subset of its solutions.

5.3. *The limit of zero entrainment*

The limit of zero entrainment ($\alpha \to 0$) is interesting, if only as a mathematical curiosity (given that the model's derivation was for the case of an entraining, turbulent plume). We note that this limit is well-defined (mathematically) in the general solution, and it is independent of which form one adopts for the function k. In this case the mass flux q is constant with height and the momentum flux reduces to

$$f = \sqrt{[2g\phi q](z - z_0)}, \tag{5.15}$$

and so we obtain density, radius and velocity:

$$\eta = \frac{q}{q+\phi}, \quad b = \frac{\sqrt{(q+\phi)}}{[2g(\phi/q)(z-z_0)]^{1/4}}, \quad w = [2g(\phi/q)(z-z_0)]^{1/2}. \tag{5.16}$$

This has a number of interesting properties. First, it is identical to the result found from a Bernoulli (i.e. quite different) approach to a non-entraining plume, discussed for example by Scorer (1978) and Fanneløp (1994). Secondly, there is always a point of zero radius ($b = 0$) on the $\alpha = 0$ solution – in sharp contrast to the case $\alpha > 0$ where such a point only exists in a subset of solutions in a particular entrainment model. Thirdly, the zero radius location for $\alpha = 0$ is at $z \to \infty$, thus constituting a point sink rather than the point source at $z = 0$ as in classic plume theory. The form of $b(z)$ predicted here has been confirmed experimentally by the small-scale low-entrainment experiments reported by Friedl, Härtel & Fanneløp (1999) (see also Friedl 1998).

The point-sink vs. point-source contrast highlights why the zero-entrainment solution cannot be obtained as a limit of the power-law solution of the Ricou–Spalding model – the general solution is required in order to form the connection. In fact if one considers the entraining solution with a neck and takes $\alpha \to 0$ with fixed q_0, then the height at which the neck occurs simply increases without limit, and the region of accelerating flow below the neck expands to fill the whole height range. Alternatively if one takes $q_0 \to 0$ with fixed $\alpha > 0$, then the neck moves down and the decelerating region above the neck is the only one which remains in the limit. Necking is thus seen as the result of a high-density-difference, low-entrainment-velocity region low down in the plume (associated with an accelerating flow) and a lower-density-difference, high-entrainment-velocity region further up.

6. Experimental data

Whilst there have been qualitative observations of plumes with area sources, and the neck is a well-known phenomenon, there is rather little precise experimental data. Here we shall look at the data we are aware of on isothermal buoyant plumes in calm conditions. Comparison with the data must be done carefully: the model is based fundamentally on arguments of self-similarity which are expected to break down close to the source, and it is therefore prudent to look primarily well above the source.

The laboratory experiments of Liedtke & Schatzmann (1997) resulted in good measurements of radial profiles for both concentration and velocity at a number of different heights. Furthermore, at all but the lowest measurement point these profiles were Gaussian to a very good approximation. At the lowest point the Gaussian

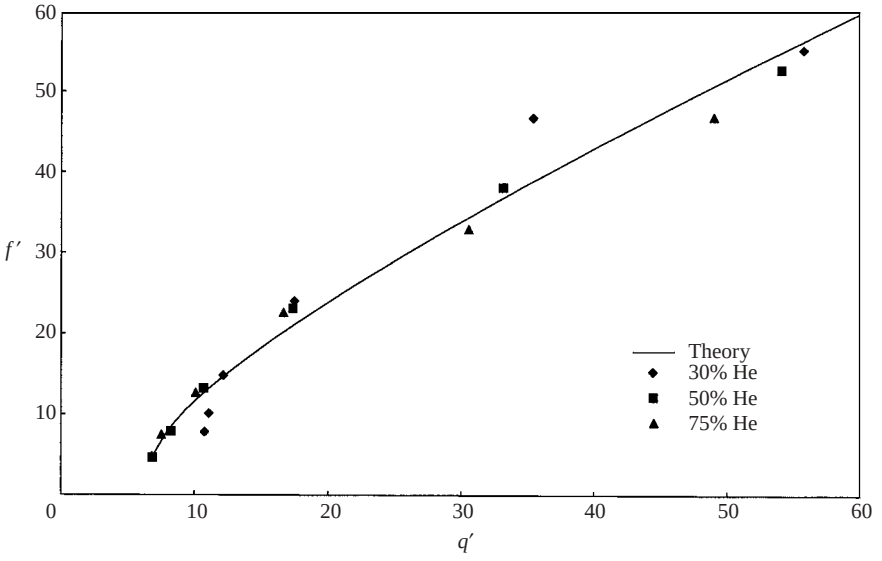

FIGURE 2. Dimensionless versions (q' and f') of the mass and momentum fluxes q and f, as extracted from the data of Liedtke & Schatzmann (points) and the fit of the Ricou–Spalding entrainment model prediction (line).

approximation was only slightly less good, showing a remaining effect of the profile at the source. Liedtke & Schatzmann fitted a fine-wire gauze across the source plane through which they released various helium–air mixtures of known concentration. The wire gauze in combination with the flow profile in the flow line, produced a turbulent plume flow with the desired properties, also quite close to the source. Webber *et al.* (1997), see also Martin *et al.* (1997), were able to take advantage of the detailed nature of the measurements to deduce model parameters as follows.

First, Gaussian curves were fitted to the measured profiles yielding centreline velocity and concentration, and radii (standard deviations of the Gaussians) for each of these profiles. The radii of the velocity and concentration distributions were not identical, but were close enough that the difference could be neglected for the purposes of the analysis. The various flux parameters (defined essentially as here in terms of the radius and centreline concentration and velocity, and therefore proportional to the integral fluxes) were then calculated from the data at each height. The buoyancy flux was immediately seen to be conserved to within 10% for all experiments over the full height range of the data (except for one maverick point). The mean for each experiment gave the buoyancy parameter (equivalent to ϕ here) for the relevant case.

Webber *et al.* then constructed the mass and momentum fluxes q and f, and in view of the simple analytic result from the Ricou–Spalding entrainment model

$$q = \sqrt{q_0^2 + \left[\frac{8\alpha}{5g\phi}\right] f^{5/2}} \tag{6.1}$$

plotted q^2 against $f^{5/2}$ and fitted a straight line. In doing so the same entrainment coefficient α was demanded for all experiments though there was no requirement that q_0 should be the same for each. The best fit when reduced to a form $f(q)$ is shown in figure 2.

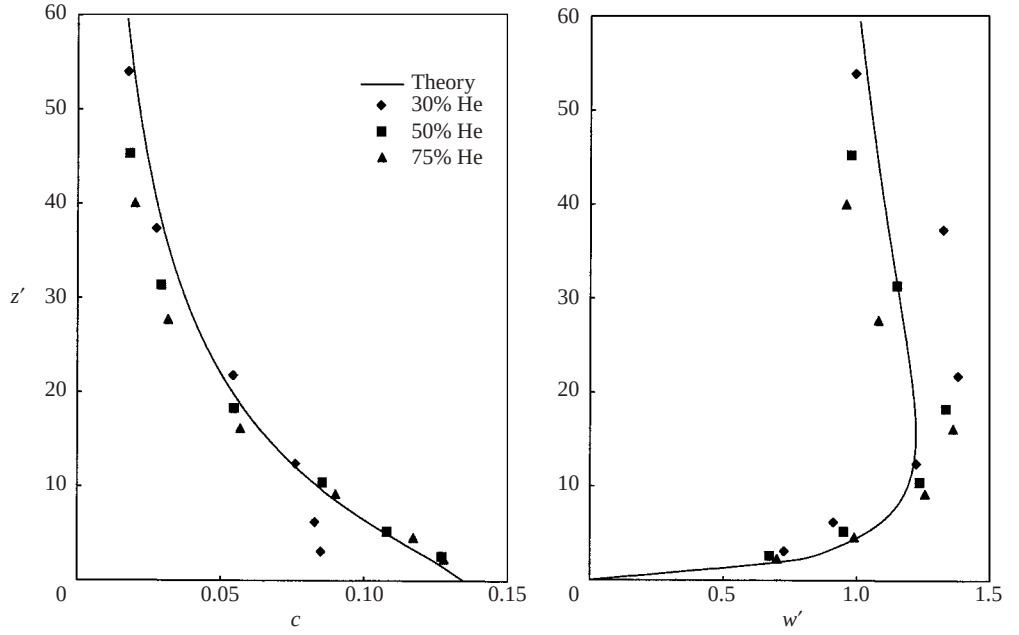

FIGURE 3. Dimensionless versions of centreline concentration and velocity as a function of height $z' = (z - z_0)/L$. The model (line) vs. the experimental data points of Liedtke & Schatzmann.

Having obtained q_0 and α in this way, the only remaining free parameter is z_0 and it was found that the best fit was almost indistinguishable from simply choosing z_0 so as to give $w(z = 0) = 0$ – these were essentially very low-momentum releases. The results for a series of experiments releasing helium at 30%, 50%, and 75% concentrations are shown in figures 3 and 4. The model is seen to fit really rather well through the neck and down to quite small height. (It could be improved by allowing for a slightly different radius of concentration and velocity profiles, as has often been found necessary.) The entrainment coefficient given by this fit was $\alpha = 0.08$, a value not far from that for a naturally turbulent plume.

The experiments of Billeter & Fanneløp (1989) were designed to study the formation of a light-gas plume in air from an underwater gas release. In their Series C, helium gas was released just below the water surface from 400 hypodermic needles spaced evenly over a circular disk of diameter 200 mm. Each needle produced a jet that broke up into a stream of tiny (1 mm) bubbles that burst when passing the water surface. The set-up was intended to produce a uniform gas source without splashing or waves. In this way it became possible to make repeatable measurements as close as one tenth of the source diameter above the water surface. The primary measurements provided profiles of the helium concentration in air as obtained with flame ionisation detectors. In all five heights were considered from 20 mm to 135 mm. Only two velocity profiles were obtained, for a different but similar case. We note that the velocity was very low and difficult to measure.

A top-hat concentration profile was expected close to the surface as a result of the uniform gas release. But all profiles including those close to source appeared to be Gaussian and could be fitted with Gaussian distributions. This is in full accord with the observations of Liedtke & Schatzmann. Furthermore, inspection of the profiles

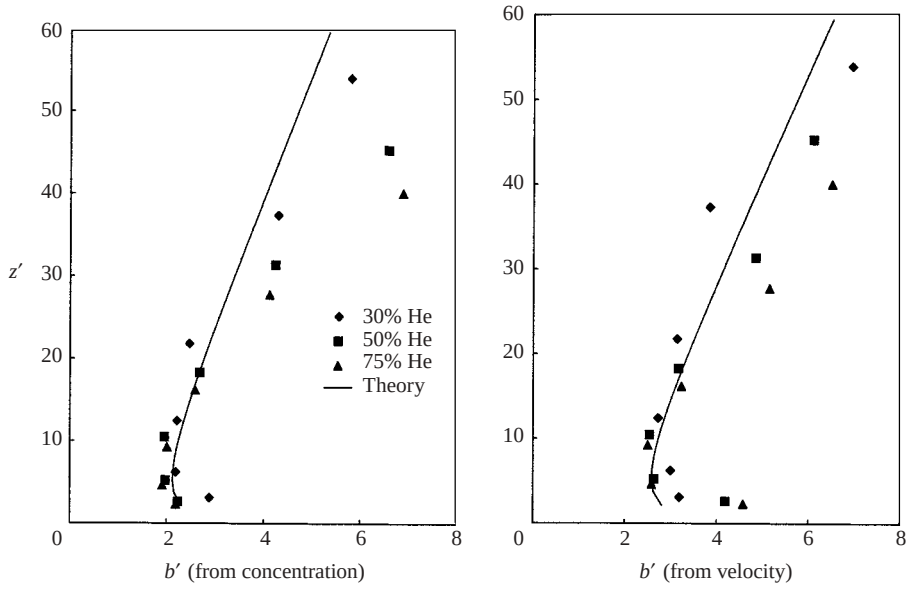

FIGURE 4. The points depict radius as extracted from the concentration velocity profiles measured by Liedtke & Schatzmann and the line the results of the model.

obtained shows a plume of contracting radius up to a height of about 90 mm, and in this region the centreline concentration remains practically constant. This indicates that profiles beneath this height represent a region of little or low entrainment for which the entrainment coefficient is rather uncertain.

The lack of velocity data and the uncertainty regarding entrainment in the near-source region, makes a comparison with our model somewhat difficult. Therefore we shall look at the centreline concentrations taken from the measurements high in the plume. Here the peak concentration starts to decrease and we apply the model to these. Our procedure is to take the data from the Gaussian fit of Billeter & Fanneløp of form

$$\hat{c}(r, z) = c(z) \exp(-r^2/2b^2) \tag{6.2}$$

and extract the centreline concentration c and radius b at each measurement height. The centreline density in the experiments is deduced from the measured centreline concentration c, giving

$$1 - \eta = (1 - \rho_{He}/\rho_a)c. \tag{6.3}$$

We assume a conserved buoyancy flux ϕ and (in the absence of velocity measurements) infer the centreline velocity from conservation of buoyancy to be

$$w = \frac{\phi}{(1 - \eta)b^2}. \tag{6.4}$$

We can now estimate the mass and momentum fluxes q and f at each measurement height as a function of the single parameter ϕ. We plot f against q (or $f^{5/2}$ against q^2) and compare with the simple formula derived from the Ricou–Spalding entrainment model.

To reduce the number of free parameters let us set the entrainment coefficient α to the value 0.08 found in the comparison with the Liedtke–Schatzmann data. In doing this we are making the assumption that, in the higher part of the plume, all memory

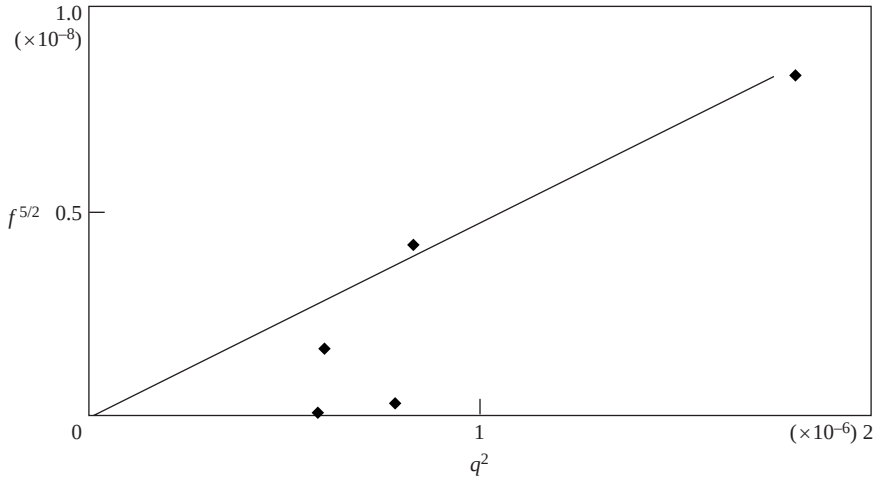

FIGURE 5. $f^{5/2}$ vs. q^2 with points extracted from the data of Billeter & Fanneløp and a linear fit to the highest points.

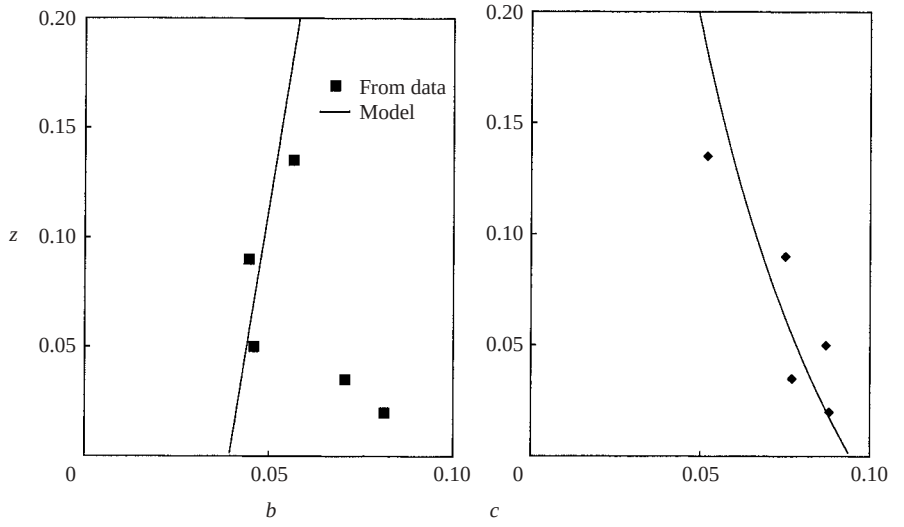

FIGURE 6. The radius of the concentration profile and the centreline concentration measured by Billeter & Fanneløp. The model results have been constrained to have $\alpha = 0.08$.

of the source is lost (and we know from the non-falling centreline concentration that this method of analysis will only work in the higher part). The comparison with $f(q)$ will then allow us to find ϕ and the other parameter q_0. The best fit to the two highest measurement points with these assumptions is shown in figure 5.

As discussed, only the two highest data points can really be included and there is not much information to be gained by fitting these with a straight line using two free parameters! However, if we translate these into curves for $c(z)$ and $b(z)$ (with an additional choice of origin) we obtain figure 6 with a reasonable fit (given the variability of the original data) to both centreline concentration and radius in the higher part.

Some comments are in order. First, if we assume that the radius of the velocity profile is the same as that of the concentration profile we can relate ϕ to the conserved integrated buoyancy flux:

$$B = 2\pi \int_0^\infty \mathrm{d}r r \left(1 - \frac{\hat{\rho}(r, z)}{\rho_a}\right) \hat{w}(r, z). \tag{6.5}$$

We find

$$\phi = B/\pi. \tag{6.6}$$

Estimating B from the helium volume flux injected gives

$$B = (1 - \rho_{He}/\rho_a)\dot{V}. \tag{6.7}$$

From these we can estimate ϕ from the source. The result is $7.4 \times 10^{-5}\,\mathrm{m^2\,s^{-1}}$ compared with $6.3 \times 10^{-5}\,\mathrm{m^2\,s^{-1}}$ derived from the above fit to the plume. The difference, roughly 15%, is not out of line with the approximations made in accepting the Gaussian profiles presented by Billeter & Fanneløp.

Secondly, it should be noted that the mass flux q that we have extracted from the data increases by less than a factor 2 from the lowest measuring point to the highest in these experiments. This can be compared with a factor of 9 in the Liedtke–Schatzmann experiments, which therefore form a stronger test of the model.

We therefore conclude that the highest part of the plume observed by Billeter & Fanneløp is consistent with the model, and consistent with the entrainment rate seen in the other experiments.

7. Discussion and conclusions

The simple model of a plume derived by Morton *et al.* (1956) relies on assumptions of self-similarity, but does not rely on a Boussinesq approximation, something which has been emphasized by Rooney & Linden (1996).

The model consists of a set of three coupled first-order differential equations and therefore the general solution depends on three parameters. For any specific solution, these must be determined from the conditions at the source. In practice this is difficult, because there is a (larger or smaller) zone immediately above the source where the self-similarity assumptions on which the model is based are not justified. Two of the three parameters are relatively straightforward: one is a buoyancy (or species) flux ϕ which is conserved on general principles through the entire plume; another is simply the freedom to choose the origin z_0. The third, q_0, is more subtle and reflects the relative magnitudes of the mass and momentum fluxes in the plume. It is difficult to relate it to measured source conditions in view of the non-self-similar zone between the MTT plume and its source.

Whether or not the solution of the equations contains a location with zero radius (a point source) depends both on the entrainment model and on the value of q_0. The Ricou–Spalding entrainment model does provide one solution (that with $q_0 = 0$) with a point source, and high enough in the plume (so that $q \gg q_0$ and $\rho \sim \rho_a$) one can find an equivalent point source which will generate the asymptotic Boussinesq solution.

The importance of the parameter q_0 and its effect on the plume structure has not been extensively examined in the literature. Morton (1959) does introduce an equivalent parameter, but only in the context of a Boussinesq approximation (which requires $q \gg \phi$ but not necessarily $q \gg q_0$). Interestingly his figure 3 shows

an accelerating–decelerating plume with a maximum in w, but, probably because he is interested in forced plumes, he does not go so far as predicting a neck with a minimum radius b within the domain of the solution.

Rooney & Linden (1996) emphasize the validity of the model's application to non-Boussinesq plumes, but their method of solution is strongly based on seeking power-law solutions, which pick out the case $q_0 = 0$ in the Ricou–Spalding entrainment model. And we argue that it is this that led them to propose that there was a theoretical basis for the Ricou–Spalding model. If one accepts that there is no reason apart from mathematical convenience to seek power-law solutions, then there is no such theoretical basis.

Hunt & Kaye (2001) follow Morton (1959) and restrict themselves to Boussinesq plumes. They define a plume with $q_0 = 0$ to be a 'pure' plume and one with $q_0 > 0$ to be a 'lazy' plume – because this implies a deficit of momentum compared with the pure plume of the same mass flux. Their prime objective is to study the effect of small values of q_0 on the position of the virtual point source to which the large-z asymptotic conical plume extrapolates back. They show that their virtual source correction markedly improves the fit to laboratory data.

Here we have examined the solutions of the plume equations in greater generality. We do not restrict ourselves either to power-law solutions or to the Boussinesq limit, and this more general view of the complete three-parameter set of solutions of the MTT model reveals a great deal. In summary:

(i) Power-law solutions only exist in specific circumstances as detailed above.

(ii) In the Ricou–Spalding entrainment model, power-law solutions form a two-parameter subset of the complete three-parameter set.

(iii) Admitting non-power-law solutions removes the theoretical basis, argued by Rooney & Linden (1996), for the Ricou–Spalding entrainment model.

(iv) The general solution includes cases where the plume first converges, and then goes through a neck and diverges again. The power-law solutions exclude these. Qualitatively at least, this behaviour is observed in real plumes, and it is of considerable practical interest.

(v) For the converging–diverging plume, there is no virtual point source (that is to say there is no point on the extrapolated solution where the radius is zero) and so any solution method which assumes one will overlook this plume geometry.

(vi) Far above the neck, the converging–diverging plume tends to the usual Boussinesq power-law solution as an asymptote. (Sufficiently high above the source, the plume becomes asymptotically close to one which *can* be generated from a point source. This simply defines an 'equivalent point source' for the asymptotic plume which gives no information about the plume structure lower down.)

(vii) The general solution is well behaved in the limit ($\alpha \to 0$) of no entrainment. In this case the height of the neck increases without limit and the converging region below the neck becomes the whole plume. All such solutions have a point sink as $z \to \infty$ – quite different in character from the point source of some of the entraining plumes.

The general converging–diverging plume solution represents a useful model of plumes from real sources, such as pool fires, burning dumps and hazardous releases of buoyant gases, as well as simulations of such events in the laboratory.

Webber *et al.* (1997) showed that the detailed experiments of Liedtke & Schatzmann (1997) could in fact be very well represented by such a model, even quite close to the source. Interestingly, Hunt & Kaye (2001) also assume that their plume solution is valid all the way down to the area source, and this is supported by their data.

The experiments of Billeter & Fanneløp (1989) were conceived differently. They were investigating the features of sub-sea natural gas releases. This is an altogether more complicated source as those authors, and Fanneløp (1994), discuss. They too see a converging–diverging plume, but one in which the centreline concentration does not decrease significantly within the converging region. The model does give a reasonable fit to the highest measurements of Billeter & Fanneløp, but overall the scale of their experiment is too small to give a good test. A more complex model allowing for deviations from self-similarity would be needed to describe these experiments better.

We would like to see more good-quality experimental data from a variety of buoyant plumes from area sources, in particular at as large a scale as possible.

REFERENCES

Billeter, L. & Fanneløp, T. K. 1989 Gas concentration over an underwater gas release. *Atmos. Environ.* **23**, 1683–1694.

Fanneløp, T. K. 1994 *Fluid Mechanics for Industrial Safety and Environmental Protection.* Elsevier.

Fanneløp, T. K., Hirschberg, S. & Kueffer, J. 1991 Surface current and recirculating cells generated by bubble curtains and jets. *J. Fluid Mech.* **229**, 629–657.

Friedl, M. J. 1998 Bubble plumes and their interactions with the water surface. Dissertation No. 12667 Swiss Fed. Inst. of Technology, ETH, Zurich.

Friedl, M. J., Härtel, C. & Fanneløp, T. K. 1999 An experimental study of starting plumes over area sources. Nuovo Cimento **22 C**, 835–845.

Hunt, G. R. & Kaye, N. G. 2001 Virtual origin correction for lazy plumes. *J. Fluid Mech.* **435**, 377–396.

Liedtke, J., & Schatzmann, M. 1997 Dispersion from Strongly Buoyant Sources. *Final Rep. EU-Project* EV5V-CT-93-0262. University of Hamburg, Meteorological Institute.

Martin, D., Webber, D. M., Jones, S. J., Underwood, B. Y., Tickle, G. A. & Ramsdale, S. A. 1997 Near- and intermediate-field dispersion from strongly buoyant sources. *AEA Tech. Rep.* AEAT/1388 on EC Research Contract EV5V-CT93-0262.

Morton, B. R. 1959 Forced plumes. *J. Fluid Mech.* **5**, 151–163.

Morton, B. R., Taylor, G. I. & Turner, J. S. 1956 Turbulent gravitational convection from maintained and instantaneous sources. *Proc. R. Soc. Lond.* A **234**, 1–23 (referred to herein as MTT).

Ricou, F. P. & Spalding, D. B. 1961 Measurements of entrainment by axisymmetrical turbulent jets. *J. Fluid Mech.* **8**, 21–32.

Rooney, G. G. & Linden, P. F. 1996 Similarity considerations for non-Boussinesq plumes in an unstratified environment. *J. Fluid. Mech.* **318**, 237–250.

Scorer, R. S. 1978 *Environmental Aerodynamics.* Ellis Horwood.

Taylor, G. I. 1958 Flow induced by jets. *J. Aerospace Sci.* **25**, 464–465.

Turner, J. S. 1973 *Buoyancy Effects in Fluids.* Cambridge University Press.

Webber, D. M., Jones, S. J. & Tickle, G. A. 1997 Dispersion in very buoyant plumes. *Hazards XIII, ICHEME Symp. Ser.* 141, pp. 89–100.